Journal of Thermal Analysis and Calorimetry, Vol. 84 (2006) 1, 213–217

ADIABATIC MEASUREMENT OF THE GIANT MAGNETOCALORIC EFFECT IN MnAs

*Leticia Tocado**, *E. Palacios and R. Burriel*

Instituto de Ciencia de Materiales de Aragón, CSIC – Universidad de Zaragoza, Pedro Cerbuna 12, 50009 Zaragoza, Spain

We have studied the compound MnAs with a giant magnetocaloric effect, which has a magneto-structural transition at 316 K. The magnetic phase diagram has been deduced from adiabatic heat-capacity measurements and from cooling and heating curves. The ferro- to paramagnetic transition changes with field from 316 K at 0 T to 335.3 K at 6 T. There is a strong thermal hysteresis between 10 and 5 K, depending on field. Direct measurements of the adiabatic temperature change caused by the application of magnetic field were made and compared with the values deduced from heat-capacity data. Moreover, adiabatic field cycles were performed quasi-statically between 0 and 6 T around the phase coexistence region, showing the strength of the effect in each phase and on the coexistence lines.

Keywords: *giant magnetocaloric effect, heat capacity, heating and cooling curves, magnetic phase diagram*

Introduction

Magnetic refrigeration is based on the magnetocaloric effect (MCE). This is an adiabatic temperature change or an isothermal entropy change of a magnetic material due to the application of a magnetic field. In the last years its importance has grown up since magnetic materials with large MCE values could be employed as magnetic refrigerants at room temperature, which is environmentally safe and energetically efficient.

In 1997, Pecharsky and Gschneidner [1] found that $Gd_5Si_2Ge_2$ exhibits a giant MCE. This compound undergoes a first-order magneto-structural transition at 276 K, which can be induced not only by changing the temperature, but also by changing the magnetic field or pressure. Other materials are being researched as an alternative to the Gd–Si–Ge family. The family $MnAs_{1-x}Sb_x$ has been reported to have a giant MCE [2]. At zero magnetic field, MnAs has a first-order transition at 316 K from ferromagnetic to paramagnetic state together with a change from hexagonal to orthorhombic structure. The compound undergoes a big volume change, $\Delta V/V=-1.7\%$, upon the transition [3] that brings a large entropy change. Using the Clapeyron equation, $dT_C/dp=\Delta V/\Delta S$, being the molar volume $V_m=2.067\cdot10^{-5}$ m^3 mol^{-1}, and $dT_C/dp=-165$ K GPa^{-1} [4], the entropy change is 16.4 J kg^{-1} K^{-1}, which makes the compound an interesting initial case for room temperature magnetic refrigeration.

The simplest experimental technique to determine ΔS_T is from magnetization measurements, using the Maxwell relation

$$\left(\frac{\partial S}{\partial H}\right)_T=\left(\frac{\partial M}{\partial T}\right)_H \Rightarrow \Delta S_T=\int_0^H (\partial M/\partial T)_H \mathrm{d}H \quad (1)$$

The magnetocaloric magnitudes ΔT_S and ΔS_T can also be obtained by integration of heat capacity at constant pressure and field, $C_{p,H}(T)$, which gives the iso-field curves in an entropy-temperature diagram,

$$S(T,H)=\int (C_{p,H}/T)\mathrm{d}T \quad (2)$$

We have obtained the MCE directly as the temperature change occurring upon the application of a magnetic field in adiabatic conditions $\Delta T(T)_{S,\Delta H}=[T(H_2)-T(H_1)]_S$ and also from heat-capacity measurements with applied magnetic field, by calculating entropy curves for different fields, and inverting the entropy function to obtain $\Delta T_S=[T(S)_{H_2}-T(S)_{H_1}]_S$.

Experimental

Heat capacity and ΔT_S have been measured at 0 and 6 T in an adiabatic calorimeter [5] provided with a superconducting coil, and in a PPMS relaxation calorimeter from Quantum Design.

A dynamic procedure has been used to map the heat capacity of sharp phase transitions with heating and cooling curves [6] at different magnetic fields. A constant temperature shift ΔT is kept between the sample holder and the adiabatic shield. Then, the sample heats or cools by radiation and conduction to the shield through the measuring wires. The rate of temperature variation is inversely proportional to the

* Author for correspondence: leticiat@unizar.es

1388–6150/$20.00

Akadémiai Kiadó, Budapest, Hungary
Springer, Dordrecht, The Netherlands

heat capacity and given by a heating or cooling power law with a conduction and a radiation term.

$$\frac{dQ}{dt}=\frac{dQ}{dT}\frac{dT}{dt}=C_{p,H}\frac{dT}{dt}$$
$$\frac{dQ}{dt}=A\Delta T+B'[(T+\Delta T)^4-T^4]\cong(A+BT^3)\Delta T \quad (3)$$

dT/dt is calculated for each point from the experimental data $T(t)$, fitting a few points around each value of T with a straight line. The constants A and B are evaluated with the results of $C_{p,H}$ obtained by the heat-pulse method at two temperatures far from the transition, where the dynamic and static points should match. Low rates are used, around dT/dt=1 mK s^{-1}, in order to assure thermal quasi-equilibrium and the temperature is recorded every 10 s.

The adiabatic temperature change has been measured upon a quasi-static application of magnetic field. The adiabatic shield follows the sample temperature with the control of an electronic PID unit which provides a thermal isolation with a drift <0.1 K h^{-1} at constant field and without external heat supply. The procedure is similar to the heat-pulse method for C_p measurements. The magnetic field is applied at a rate of 0.01 T s^{-1}, and waits 3 min for thermal equilibrium at the final field. The temperature increment is obtained extrapolating the thermal evolution at the constant initial and final fields to the central time of the field change. The adiabatic temperature increment, ΔT_S, is measured with a typical accuracy of about 10 mK. An adiabatic magnetization process in several field steps is shown in Fig. 1.

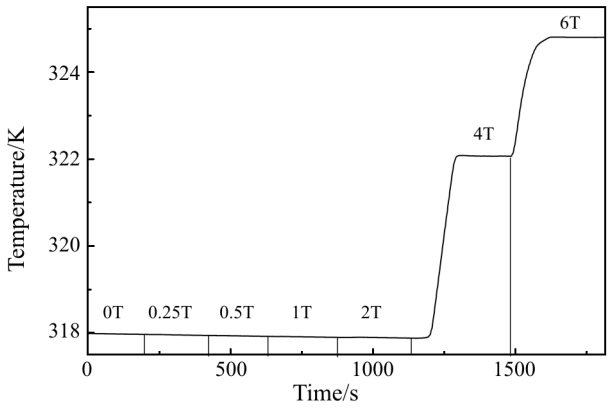

Fig. 1 Experimental adiabatic magnetization process in steps of magnetic field

The magnetization process is adiabatic for the complete system, sample holder plus sample. The temperature of the system increases $\Delta T_{exp}=T_2-T_1$. The entropy variation of the sample holder is $\Delta S_h=S_h(T_2)-S_h(T_1)$ and the sample experiences an entropy variation $-\Delta S_h$. The entropy of the sample holder is obtained by integration of C_p/T, from the experimental data of the empty holder. The values ΔT_{exp} have to be corrected for this entropy change in order to obtain the adiabatic temperature increment of the sample, ΔT_S. Two procedures used for this correction are described in the next section.

Results and discussion

The adiabatic heat capacity at zero field displayed an anomaly at 320 K in a first run from 80 to 340 K. Subsequent runs showed the transition at a lower temperature, T_C=316 K (Fig. 2). This shift of the transition temperature was also observed in magnetic measurements [7], and may be due to a curing process produced by heating-cooling cycles applied to the fresh sample. This anomaly corresponds to a first-order transition from ferromagnetic to paramagnetic phase simultaneously with a change from hexagonal to orthorhombic structure. Heat-capacity measurements were made in a PPMS between 4.5 and 120 K at zero field. These data agree with the adiabatic results in the overlapping range, from 80 to 120 K, with accuracy better than 0.6%.

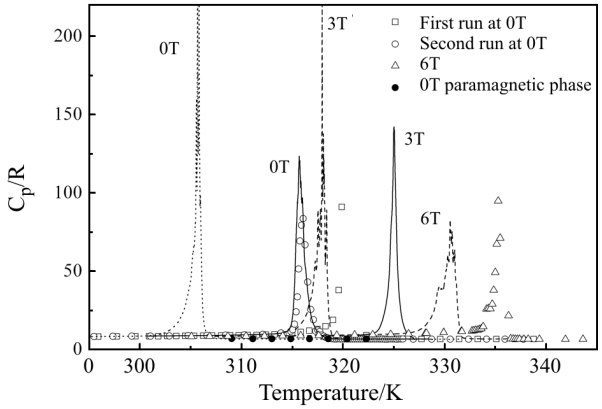

Fig. 2 Heat-capacity data for a constant magnetic field: heat-pulse method (symbols), cooling curves (discontinuous lines) and heating curves (continuous lines)

A cooling curve showed a thermal hysteresis of 10 K. After cooling from the paramagnetic-orthorhombic phase to 307 K, just above the cooling transition temperature, the heat capacity was measured up to 322 K obtaining the non-anomalous baseline (full circles in Fig. 2).

The enthalpy of the transition at zero field was calculated from a broad temperature step covering the whole peak (enthalpy run). The resulting value for the transition enthalpy is 1004 J mol^{-1} and the transition entropy 24.46 J $kg^{-1}K^{-1}$, slightly higher than the results reported in [8]. They were also obtained by integration of the adiabatic heat-capacity data and the

thermal curves. The enthalpy of the heating curve agrees with the value from the enthalpy run and both are higher than the values determined from the heat-pulse data. This compound has a sharp first-order transition presenting avalanche effects, and the relaxation time required after a heat pulse in the transition is very long. Due to that, the $C_{p,H}$ values from the heat-pulse method are underestimated and the same happens for the resulting transition entropy and enthalpy.

The heat capacity at 6 T also shows a sharp anomaly, displaced to 335 K and presenting a shoulder at 334 K. A thermal hysteresis of 4.6 K was observed from the cooling curve at 6 T.

Heating and cooling curves were made for applied fields between 0 and 6 T in order to obtain the heat capacity as explained before (Fig. 2). Some thermal curves have multiple peaks due to an avalanche effect, typical for first-order transitions.

The transition temperatures, enthalpies and entropies were obtained for several applied magnetic fields and are listed in Table 1. The main features observed are: (*i*) the transition temperature increases with the magnetic field, (*ii*) there is thermal hysteresis that decreases with the magnetic field and, (*iii*) the transition entropy and enthalpy decrease with the magnetic field in both heating and cooling measurements. Figure 3 shows the magnetic phase diagram, deduced from $C_{p,H}$ data. It shows two straight lines which define the ferro- to paramagnetic transition, 'heating line', and the para- to ferromagnetic transition, 'cooling line'. The position of these lines is quite independent of the heating or cooling rate and indicates the borders of the stability domain for each phase. In the region between the lines there is bistability and the actual phase depends on the thermal history. Our magnetic phase diagram agrees with the one obtained in [3] from magnetization and volume change, that shows the two-phase lines converging at a critical point near 365 K and 9.5 T, where the transition should become second order.

To analyze the thermal process of the sample when a magnetic field is applied around the phase coexistence region, adiabatic field cycles were measured varying the magnetic field slowly, at 3.6 mT s^{-1} (Fig. 3). The first cycle was performed starting at 318 K and increasing the field from 0 T. The sample

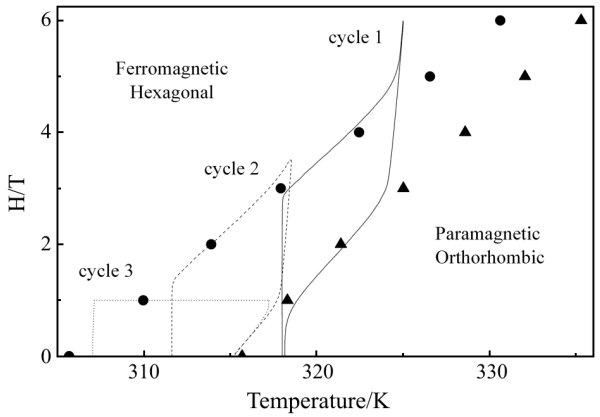

Fig. 3 Magnetic phase diagram: field cycles (lines), ferrro- to paramagnetic transition (triangles) and para- to ferromagnetic transition (circles)

Table 1 Transition temperatures, enthalpies and entropies at various fields

	H/T	T_C/K	ΔH/J mol^{-1}	ΔS/J kg^{-1} K^{-1}	Type of data
Heating	0		1004(5)	24.46	enthalpy run
	0	315.7(1)	1002(5)	24.4	heating curve
	0	316.1(1)	800(200)	20	heat pulse
	1	318.3(2)	927(5)	22.41	heating curve
	2	321.5(2)	888(5)	21.26	heating curve
	3	325.0(1)	854(5)	20.23	heating curve
	4	328.6(1)	805(5)	18.89	heating curve
	5	332.1(2)	762(5)	17.67	heating curve
	6	335.3(2)	731	16.77	heat pulse
Cooling	0	305.7(1)	1226(5)	30.86	cooling curve
	1	310.0(2)			cooling curve
	2	313.9(1)	1105(5)	27.08	cooling curve
	3	318.0(3)			cooling curve
	4	322.5(2)			cooling curve
	5	326.7(5)	932(5)	21.96	cooling curve
	6	330.7(5)	879(5)	20.5	cooling curve

remains initially in the paramagnetic phase, where there is not MCE. When the magnetic field reaches the para- to ferromagnetic transition line, around 3 T, the sample starts to convert to the ferromagnetic phase, and the temperature increases at 4.16 K T^{-1} (magnetocaloric effect). During this conversion process the two phases coexist and the sample moves along the para-ferro phase line with the magnetic field increase. The thermal evolution does not exactly coincide with the para-ferro phase line due to the finite width of the C_p peak. The phase conversion starts slightly below the para-ferro phase line and finishes slightly above. When the whole sample has been converted, at about 5 T and 325 K, the MCE is the normal one for a ferromagnet, approximately linear, with a small magnetic field dependence, dT/dH=0.3 K T^{-1}. When the magnetic field is removed the sample remains in the ferromagnetic phase down to reaching the ferro-para phase line, at around 3 T and 324 K, where the sample starts to convert to the paramagnetic phase, going along the transition line while the two phases coexist. The temperature decreases (magnetocaloric effect) at 3.34 K T^{-1}. The sample is in the paramagnetic phase when it reaches 1 T at 318 K, and drops almost vertically without magnetocaloric effect. For the second cycle (dashed line in Fig. 3), the initial state was reached by cooling from the paramagnetic phase and starting at 311.6 K. The final state is, at H=0 and T_C, a mixture of the two phases. The same final state in the H–T diagram was reached by another cycle (dotted line in Fig. 3). The initial state was reached by heating from the ferromagnetic phase up to 307 K. At this temperature a magnetic field was applied up to 1 T. The sample was heated to 317 K in a constant field of 1 T, where the magnetic field was removed in adiabatic conditions. The temperature decreases at 3.34 K T^{-1} down to T_C along of the ferro-para phase line, being the final state a mixture of phases.

The direct measurements of ΔT_S have been performed by applying consecutive fields of 0–0.25–0.5–1–2–4–6 T. An independent run was performed with the steps 0–3 T–0. Magnetocaloric effect is not observed for magnetic fields smaller than 3 T. The magnetic phase diagram shows that the MCE starts at a threshold field of around 2.5 T at T_C.

There are two ways to correct ΔT_{exp} for the effect of the entropy gained by the sample holder. The experimental data of the direct adiabatic temperature increment is $\Delta T_{exp}=T_2-T_1$ when varying the magnetic field from H_1 to H_2. First, if the initial entropy of the sample, $S_1=S(T_1,H_1)$, is known from previous C_{p,H_1} data (Eq. (2)), the entropy at T_2 and H_2 is $S_2=S(T_2,H_2)=S_1-\Delta S_h$. This value can be calculated for each experimental point, ΔT_{exp}, and the entropy curve as a function of temperature can be delineated for the new field H_2. Then, the real adiabatic temperature increment for the sample is deduced as the difference $\Delta T_S=T_3-T_1=T(S_1,H_2)-T(S_1,H_1)$, (Fig. 4). The second possibility is to make the correction using the entropy at the final magnetic field, which corresponds to the final state of the sample in the phase diagram (see in Fig. 4 an example for a temperature increment from T_1' to T_2'). The enthropy of the cooling process $S(T,H_2)$ is known from C_{p,H_2} (cooling curve in magnetic field). The heating C_{p,H_2} data should not be used because they correspond to the ferro- to paramagnetic phase transition, while the field cycles prove the transition to occur at the cooling line. Using the experimental T_2', H_2 and $\Delta S_h'$ imposing the condition $S(T_2',H_2)+\Delta S_h'=S(T_3',H_2)$, the final temperature, T_3', for an adiabatic process is determined. Both correction methods give the same results, within the experimental resolution, when there is not a sharp phase transition or the transition is fully achieved during the field application. When the initial or final state is a mixture of the two phases the entropy is not known with precision at a particular temperature and small errors in temperature produce severe errors in the determination of the entropy. When the initial state is a mixture of phases we chose the second method for the correction, and the first one is selected when the final state happens to be a mixture of phases.

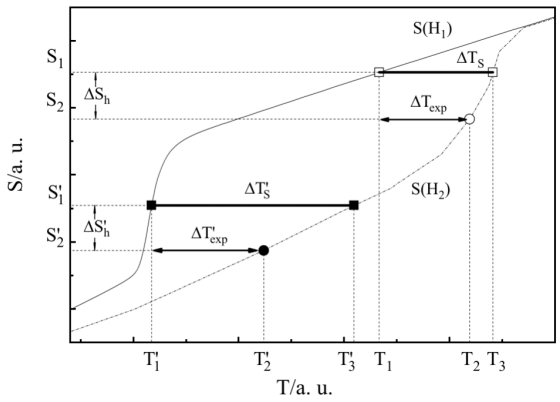

Fig. 4 Correction of the entropy gained by the sample holder: first method (open symbols) and second one (full symbols)

The direct measurements ΔT_{exp} have been corrected and the results for ΔT_S with different field increments from 0 to $H\leq 6$ T are represented in Fig. 5. They show an abrupt jump near 316 K, reaching a maximum value 12.4 K at T=318 K for ΔH=6 T, and then decreasing smoothly to zero for higher T.

The entropy curves for different magnetic fields have been calculated by integration of $C_{p,H}$ (Eq. 2). At zero magnetic field, the entropy has been obtained between 4.5 and 340 K, from the heat-pulse and relaxation

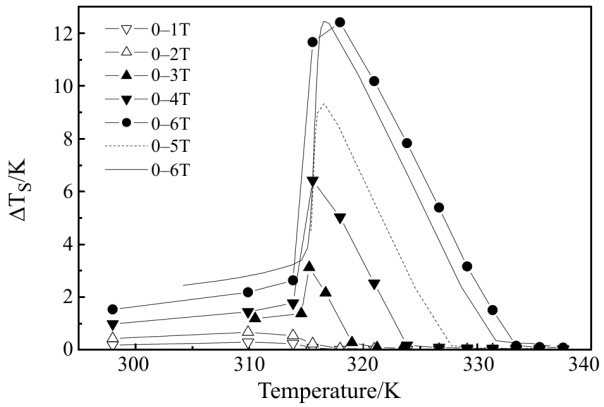

Fig. 5 Direct magnetocaloric effect (connected symbols), and curves obtained from $C_{p,H}$ data (lines)

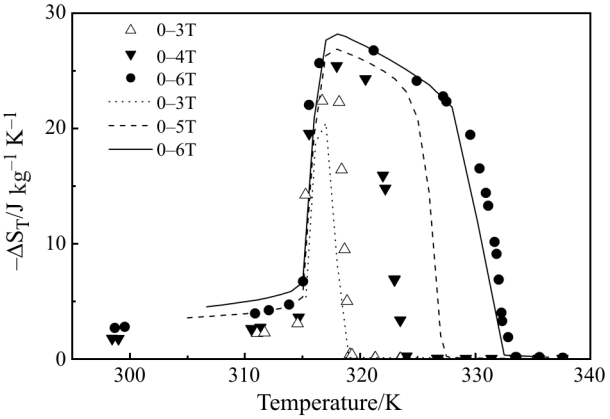

Fig. 6 ΔS_T deduced from $C_{p,H}$ data (lines) and direct ΔT_S (symbols)

C_p measurements. Lacking data from low temperatures for the different magnetic fields, we have adjusted the entropy curve making $T(S,H)=T(S,H=0)+\Delta T_S$ in the high temperature region, where the adiabatic temperature increment is very small. $T(S,H)$ is the inverse function of $S(T,H)$ and ΔT_S has been obtained from direct measurements corrected for the effect of the holder by the first method.

From the entropy curves at 0 T in heating and at H_2 in cooling, the values of ΔT_S and ΔS_T have been determined for different magnetic field increments. ΔT_S deduced from $C_{p,H}$ (Fig. 5) have the same shape than the direct ΔT_S. The slight differences are due to the small errors of the indirect determination. ΔS_T has also been deduced from the entropy curve at zero field and the direct data of ΔT_S (Fig. 6), obtaining a good agreement. For ΔH=6 T, ΔS_T shows a plateau between 316 and 330 K, with a maximum of 28.2 J kg^{-1} K^{-1}.

Conclusions

We have determined the magnetic phase diagram from heat-capacity measurements in heating and cooling using heat pulses and thermal curves at several constant magnetic fields.

The direct measurement of ΔT_S for quasi-static variations of the field is a very precise technique and the two ways used to correct the entropy gained by the sample holder avoid errors in the coexistence phase regions.

The compound MnAs has a giant magnetocaloric effect associated to a first-order magnetostructural transition and a strong dependence with the magnetic field has been found $d(\Delta T_S)/dH$=4.16 K T^{-1}. ΔS_T is higher than the value found in $Gd_5Si_2Ge_2$ for ΔH=5 T. But MnAs also presents a strong magnetic and thermal hysteresis making the MCE to appear only for magnetic fields higher than 2.5 T above T_C. The hysteresis decreases its possibilities for application in magnetic refrigeration.

Acknowledgements

This work has been funded by the Spanish Ministerio de Educación y Ciencia and FEDER, projects MAT2001-3507-C02-02 and MAT2004-03395-C02-02.

References

1 V. K. Pecharsky and K. A. Gschneidner Jr., Phys. Rev. Lett., 78 (1997) 4494.
2 H. Wada, T. Morikawa, K. Taniguchi, T. Shibata, Y. Yamada and Y. Akishige, Physica B, 328 (2003) 114.
3 A. Zieba, Y. Saphira and S. Foner, Phys. Lett., 91A (1982) 243.
4 N. Menyuk, J. A. Kafalas, K. Dwight and J. B. Goodenough, Phys. Rev., 177 (1969) 942.
5 F. Pavese and V. M. Malyshev, Adv. Cryog. Eng., 40 (1994) 119.
6 E. Palacios, J. J. Melero, R. Burriel and P. Ferloni, Phys. Rev. B, 54 (1996) 9099.
7 L. Tocado, unpublished data.
8 H. J. Krokoszinski, C. Santandrea, E. Gmelin and K. Bärner, Phys. Status Solidi, 113 (1982) 185.

DOI: 10.1007/s10973-005-7180-z